On the Coexistence of Multi-Static Tracking Radars with Cell Free Massive MIMO

Aparna Mishra†, Ribhu Chopra†, Bhavani Shankar M. R.*
† Department of EEE, IIT Guwahati, Guwahati, Assam, India.
* University of Luxembourg, Luxembourg City, Luxembourg.
Emails: {m.aparna,ribhufec}@iitg.ac.in,bhavani.shankar@uni.lu

***Abstract*—In this paper, we evaluate the performance of a coexistence based integrated communications and sensing (ICS) system, combining a cell free massive multiple input multiple output (CF-mMIMO) system with a multi-static sensing radar. The multi-static radar is assumed to consist of multiple sensors, all tracking a single target and connected to a fusion centre (FC). The radar subsystem is further assumed to employ a two level extended Kalman filter (EKF) that performs the tracking at both the individual sensors and at the FC. The communications subsystem is assumed to consist of the uplink of a CF-mMIMO system and its operation is divided into two sub-frames, viz. channel estimation and data transmission. We evaluate the system performance in terms of the achievable rates by the communication subsystem and the mean square error (MSE) tracking performance of the radar subsystem. Via extensive numerical simulations, we show that due to the increased diversity offered by distributed nature of both the subsystems, they are able to coexist without causing significant deterioration in each other's performance.**

***Index Terms*—Integrated Communications and Sensing, Performance Analysis, Cell Free Massive MIMO, Extended Kalman Filter, Multi-Static Radar**

I. INTRODUCTION

The recent developments in communications and sensing systems, coupled with the advent of intelligent transportation systems (ITS), or smart vehicles have actively propelled the idea of integrated communication and sensing (ICS) systems [1]–[4]. These systems have been shown to offer reduced hardware costs, in addition to increased spectral efficiency, and have recently become an active research area [5]. Presently, the design of ICS systems is approached via one of the three design philosophies, viz., co-existence, cooperation, and co-design [6]. Out of these, the co-design approach while offering optimized performance for both the communications and radar subsystems, is considered impractical due to its incompatibility with legacy systems [7]. Whereas, the co-existence based approach, that treats the two subsystems as potential sources of interference for each other, is preferable for implementation with legacy systems [7], [8]. Therefore, in this paper, our focus is on the performance analysis of an ICS system consisting of a cell free massive multiple input multiple output (CF-mMIMO) system coexisting with a multi-static tracking radar.

One of the first works exploring the idea of coexistence based ICS systems was [9], wherein the opportunistic co-existence of a rotating radar with a cognitive communication system was analysed. Following this, the idea of null space projection (NSP) for coexistence based ICS systems was explored in [10] and references therein. The authors in [6], [11] have considered the ICS system as a medium access control (MAC) channel and derived bounds on the system performance in terms of achievable rate regions. In this context [6], [11] also define the notion of the radar rate as a metric to evaluate the achievable radar performance. More recently, ICS systems that integrate radars with the state of the art technologies for implementing the physical layer of wireless communication systems such as mMIMO [12] and CF-mMIMO systems [13] have also been considered [7], [8], [14].

In this context, CF-mMIMO is considered a key enabling technology for the physical layer of beyond 5G (B5G) and 6G wireless communications systems. This is because it offers near uniform coverage to all the users while inheriting the advantages of cellular mMIMO such as power scaling, and high spectral and energy efficiencies [15], [16]. Therefore, the idea of ICS systems built around a CF-mMIMO system have recently been explored [13]. However, all these works focus on a co-design approach, and discuss algorithms to optimize the joint operation of the system. Moreover, to the best of our knowledge, there exists no literature on the co-existence of a CF-mMIMO system with a radar. Therefore, in this paper we analyse the performance of a co-existence based ICS system comprising a multi-static tracking radar and a CF-mMIMO system. Our precise contributions to the study of this system are listed as follows.

1) We derive the tracking equations for the Extended Kalman filter (EKF) based tracking radar for both the individual radar sensors as well as the FC considering the interference from the communications subsystem. We also use analyse the tracking performance of the underlying EKF, at the sensors and the FC in terms of the corresponding MSE matrices.
2) We evaluate the uplink channel estimation performance of the communication subsystem in the presence of the radar generated interference in terms of the mean squared channel estimation error.
3) Using these channel estimates, we derive an expression for the instantaneous achievable rate for each user in the communication subsystem.

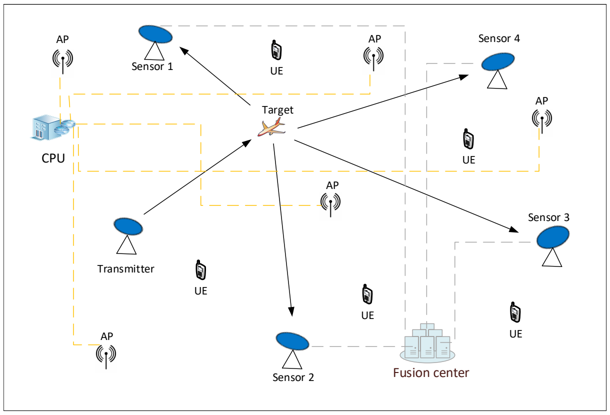

Fig. 1: System Model

4) Finally, via detailed numerical simulations we evaluate the system performance for different parameters such as the operating powers of the two subsystems. We also use these results to evaluate the potential operating points of the system and identify the underlying trade-offs.

The key takeaway of this work is that a multi-static radar can co-exist with a CF-mMIMO system without causing much deterioration to the performance of either of the two subsystems. We introduce the system model considered by us in the next section.

II. System Model

As shown in Fig. 1, we consider a CF-mMIMO communication system including N access points (APs), each having M_a antennas and serving K single antenna users in coexistence with a multi-static radar having an M_t antenna transmitter and L single antenna sensors connected to a FC. The multi-static radar is tracking a target moving at a fixed but unknown velocity. Both the communication system and the radar simultaneously operate over the same spectrum resources. All the APs in the communications subsystem are connected to a central processing unit (CPU) via instantaneous fronthaul links, and are assumed to be fully synchronized. Similarly, all the sensors in the radar subsystem are connected to the FC via an instantaneous wire-line additive white Gaussian noise (AWGN) channel. In the next sub-sections we describe the system and signal models for both the communication and the sensing subsystems.

A. The Communication Subsystem

We assume the communication subsystem to operate in the time division duplexed (TDD) mode with all the APs simultaneously serving all the K users, at a carrier frequency f_c over a common spectrum. The channels between the APs and the users are assumed to be frequency flat rich scattering. Let $\sqrt{\beta_{ik}}\mathbf{h}_{ik} \in \mathcal{C}^{M_a \times 1}$ denote the channel between the ith AP and the kth user, with $\sqrt{\beta_{ik}}$ and $\mathbf{h}_{ik} \sim \mathcal{CN}(\mathbf{0}, \mathbf{R}_{ik})$ respectively representing the slow and fast fading components.

The communication frame is divided into two sub-frames viz. training and data transmission. During the first sub-frame, the users transmit pilots to the APs that are used by the latter to estimate the underlying channels. Following this, during the data transmission subframe, the UEs transmit uplink data towards the APs, that is detected by the latter using the available channel estimates.

Letting the kth UE transmit the symbol $x_k[n]$ with energy $\epsilon_{x,k}$ at the nth time instant, we can write the signal received by the ith AP, in the absence of radar generated interference as

$$\mathbf{z}_i[n] = \sum_{k=1}^{K} \sqrt{\beta_{ik}}\mathbf{h}_{ik} x_k[n] + \boldsymbol{\omega}_{a,i}[n] \tag{1}$$

where $\boldsymbol{\omega}_{a,i}[n] \in \mathcal{C}^{M_a \times 1}$ denotes the AWGN at the ith access point. Following this, the APs forward their signals to the CPU, that is assumed to possess the channel state information (CSI) estimates for minimum mean square error (MMSE) combining based data detection [16].

B. The Sensing Sub-system and Target Tracking Model

We assume that the L radar sensors jointly detect and track a moving target using multi-static sensing [17]. These sensors are further connected to a FC for signal synchronization and joint processing.

In the absence of any communication subsystem generated interference, the sensing signal received by the lth sensing receiver, at the nth time instant can be expressed as

$$\xi_l[n] = h_{r,l} e^{j2\pi f_{d,l}(n-n_l)} a(\theta_l)\mathbf{a}^H(\theta_t)\boldsymbol{\zeta}[n-n_l] + \omega_{r,l}[n] \tag{2}$$

where $h_{r,l}$ is the zero mean circularly symmetric complex Gaussian (ZMCSCG) distributed target to sensor channel coefficient, θ_l is the angle of arrival at the lth sensor and $a(\theta_l)$ is the corresponding antenna response, θ_t is the angle of departure from the transmitter and $\mathbf{a}(\theta_t)$ is the corresponding antenna array response vector, incorporating the effects of random radar cross section and path loss, $f_{d,l}$ is the Doppler frequency shift as seen by the lth sensor, n_l is the time delay corresponding to lth sensor, $\boldsymbol{\zeta}[n]$ is the deterministic radar transmit signal at nth time instant having a transmit power P_t, and $\omega_{r,l}[n]$ is the AWGN having variance $\sigma^2_{r,l}$.

The state of target at the nth time instant is given as $\mathbf{s}[n] = [r_x[n], r_y[n], v_x[n], v_y[n]]^T$, where the pairs $(r_x[n], r_y[n])$, and $(v_x[n], v_y[n])$ respectively denote the target's position and velocity in the Cartesian coordinate system. Following the discrete state transition model [18], the state of the target at the nth adaptation cycle can be written as

$$\mathbf{s}[n] = \mathbf{A}\mathbf{s}[n-1] + \mathbf{w}_s[n] \tag{3}$$

where $\mathbf{A} = [\mathbf{T} \otimes \mathbf{I}_2]$ is the state transition matrix, with $\mathbf{I}_K$ representing the order K identity matrix, $\mathbf{T} = \begin{bmatrix} 1 & \mathit{\Delta} \\ 0 & 1 \end{bmatrix}$, $\mathbf{w}_s[n]$ being the Gaussian distributed process noise having a covariance matrix $\mathbf{R}_s$, and $\mathit{\Delta}$ is the time period of the adaptation cycle.

C. Interference Channel Models

We assume that the interference channel between the radar transmitter and the ith AP is $\mathbf{G}_{ri} \in \mathcal{C}^{M_a \times M_t}, i \in$

$\{1, 2, \ldots, N\}$. The entries of $\mathbf{G}_{ri}$ are assumed to be independent and identically distributed (i.i.d.) ZMCSCG random variables having variances $\eta_{Ii} = \min(d_{ri}^{-\alpha}, 1)$ with α = 3.6 such that d_{ri} is the distance between the radar transmitter and ith AP. Additionally, we assume that the MMSE estimates of $\mathbf{G}_{ri}$, given by $\hat{\mathbf{G}}_{ri}$ are available at the CPU, such that

$$\mathbf{G}_{ri} = \hat{\mathbf{G}}_{ri} + \tilde{\mathbf{G}}_{ri}, \tag{4}$$

with $\tilde{\mathbf{G}}_{ri}$ being the estimation error matrix whose entries are orthogonal to the corresponding entries of $\hat{\mathbf{G}}_{ri}$. The entries of $\tilde{\mathbf{G}}_{ri}$ are also i.i.d. Gaussian and are assumed to have a variance η_{ei}. In case the estimate of an interference channel is not available at the CPU, we set $\hat{\mathbf{G}}_{ri} = 0$, and $\eta_{ei} = \eta_{Ii}$. Similarly, the interference channel between kth UE and lth sensor is denoted by g_{kl}, $k \in \{1, 2, \ldots, K\}$ and $l \in \{1, 2, \ldots, L\}$. The entries of g_{kl} are assumed to be i.i.d ZMCSCG having a variance of η_{kl} that is equal to the large scale fading coefficient between kth user and lth sensor. No information about this channel is assumed at the radar sensors.

III. Target Tracking

At each sensing instant, the radar subsystem follows a two step procedure for tracking. During the first step the sensor nodes use the most recent observation to update their respective state estimates, and transmit those to the FC. During the second step the FC assimilates the state estimates from all the sensor nodes to obtain the overall state estimate. In this section, we elaborate on these two steps.

A. Tracking at the lth sensor node

The signal received by the lth sensing receiver, at the nth time instant, in the presence of communication interference can be expressed as,

$$\xi_l[n] = h_{r,l} e^{j2\pi f_{d,l}(n-n_l)} a(\theta_l) \mathbf{a}^H(\theta_t) \boldsymbol{\zeta}[n-n_l] + \sum_{k=1}^{K} g_{kl} x_k + \omega_{r,l}[n]. \tag{5}$$

This can be used to extract the parameter vector $\mathbf{y}_l[n]$ comprising the range, angle and relative speed of the target, that can be expressed as a function of the underlying state $\mathbf{s}[n]$ as,

$$\mathbf{y}_l[n] = \mathbf{f}_l(\mathbf{s}[n]) + \mathbf{w}_{y,l}[n], \tag{6}$$

where $\mathbf{w}_{y,l}[n] \sim \mathcal{N}(\mathbf{0}, \boldsymbol{\Lambda}_{y,l}[n])$, is the observation noise, and $f_l(.)$ is the measurement function expressed as,

$$f_l(\mathbf{s}[n]) = [R_l[n], \theta_l[n], \nu_l[n]]^T = \begin{bmatrix} \sqrt{(r_x[n]-q_{l,x})^2 + (r_y[n]-q_{l,y})^2} \\ \tan^{-1}\left[\frac{r_y[n]-q_{l,x}}{r_x[n]-q_{l,y}}\right] \\ \frac{(r_x[n]-q_{l,x})v_x[n] + (r_y[n]-q_{l,y})v_y[n]}{\sqrt{(r_x[n]-q_{l,x})^2 + (r_y[n]-q_{l,y})^2}} \end{bmatrix} \tag{7}$$

with $(q_{l,x}, q_{l,y})$ representing the location of lth sensor node in Cartesian coordinates, $R_l[n], \theta_l[n]$ and $\nu_l[n]$ respectively being are the target's range, azimuth and velocity. We also note that the matrix $\boldsymbol{\Lambda}_{y,l}[n]$ takes the form

$$\boldsymbol{\Lambda}_{y,l}[n] = \mathrm{diag}(\sigma_{R,l}^2[n], \sigma_{\theta,l}^2[n], \sigma_{\nu,l}^2[n]). \tag{8}$$

Here, $\sigma_{R,l}^2[n], \sigma_{\theta,l}^2[n]$ and $\sigma_{\nu,l}^2[n]$ are the Cramer-Rao lower bounds on the mean squared estimation error for $R[n], \theta[n]$ and $\nu[n]$ respectively, and are expressed as [19] [20],

$$\sigma_{R,l}^2[n] = \frac{\sum_{k=1}^{K} \epsilon_{x,k}\eta_{kl} + \sigma_{r,l}^2}{h_{r,l}^2 P_t} B^{-2} c_R,$$
$$\sigma_{\theta,l}^2[n] = \frac{\sum_{k=1}^{K} \epsilon_{x,k}\eta_{kl} + \sigma_{r,l}^2}{h_{r,l}^2 P_t} \theta_b^2 c_\theta,$$
$$\sigma_{\nu,l}^2[n] = \frac{\sum_{k=1}^{K} \epsilon_{x,k}\eta_{kl} + \sigma_{r,l}^2}{h_{r,l}^2 P_t} B^2 c_\nu \tag{9}$$

with B and θ_b being the radar's transmit signal bandwidth and the lth sensor's receive beam-width respectively, and c_R, c_θ, c_ν being constants.

We let $\hat{\mathbf{s}}[n-1|n-1]$ denote the MMSE estimate of the state vector at the $(n-1)$th instant, based on the observations till the $(n-1)$th instant. We let $\mathbf{M}[n-1|n-1] = E[(\mathbf{s}[n-1] - \hat{\mathbf{s}}[n-1|n-1])(\mathbf{s}[n-1] - \hat{\mathbf{s}}[n-1|n-1])^H]$ denote the corresponding MSE matrix. Now, the predicted state vector at the nth instant takes the form $\hat{\mathbf{s}}[n|n-1] = \mathbf{A}\hat{\mathbf{s}}[n-1|n-1]$. Based on this, the MMSE estimate $\hat{\mathbf{y}}_l[n|n-1]$ of $\mathbf{y}_l[n]$, can be expressed as, $\hat{\mathbf{y}}_l[n|n-1] = f_l(\hat{\mathbf{s}}[n|n-1])$ Similarly, the prediction MSE matrix for the nth adaptation cycle, based on the observations till the $(n-1)$th instant takes the form

$$\mathbf{M}[n|n-1] = \mathbf{A}\mathbf{M}[n-1|n-1]\mathbf{A}^H + \mathbf{R}_s[n]. \tag{10}$$

We assume that $\hat{\mathbf{s}}[n|n-1]$ and $\mathbf{M}[n|n-1]$ are all made available at all the sensors by the FC.

Consequently, the innovation component during the nth adaptation cycle is given by, $\boldsymbol{\alpha}_l[n] = \mathbf{y}_l[n] - \hat{\mathbf{y}}_l[n|n-1]$. It is easy to show that the covariance matrix of $\boldsymbol{\alpha}_l[n]$ is

$$\mathbf{R}_{\alpha,l}[n] = \left(\mathbf{F}_l[n]\mathbf{M}[n|n-1]\mathbf{F}_l^H[n] + \sum_{k=1}^{K} \epsilon_{x,k}\eta_{kl}\mathbf{I}_{N_r} + \boldsymbol{\Lambda}_{y,l}[n]\right), \tag{11}$$

where $\mathbf{F}_l[n] = \frac{\partial f_l}{\partial \mathbf{s}[n]}\Big|_{\mathbf{s}[n]=\hat{\mathbf{s}}[n|n-1]}$. Based on this, we can write the Kalman filtering gain at the lth sensor as

$$\boldsymbol{\Gamma}_l[n] = \left(E[\mathbf{s}[n]\boldsymbol{\alpha}_l[n]]\right)\mathbf{R}_{\alpha,l}^{-1}[n] = \left(\mathbf{M}[n|n-1]\mathbf{F}_l^H[n]\right) \times \left(\mathbf{F}_l[n]\mathbf{M}[n|n-1]\mathbf{F}_l^H[n] + \sum_{k=1}^{K} \epsilon_{x,k}\eta_{kl}\mathbf{I}_{N_r} + \boldsymbol{\Lambda}_{y,l}[n]\right)^{-1}. \tag{12}$$

Following this, the filtered state vector by the lth sensor node for the nth adaptation cycle is given by

$$\hat{\mathbf{s}}_l[n|n] = \hat{\mathbf{s}}_l[n|n-1] + \boldsymbol{\Gamma}_l[n]\boldsymbol{\alpha}_l[n], \tag{13}$$

and the MSE matrix of filtered state, at the lth node $\mathbf{M}_l[n|n] = E[(\mathbf{s}[n] - \hat{\mathbf{s}}_l[n|n])(\mathbf{s}[n] - \hat{\mathbf{s}}_l[n|n])^H]$ takes the form

$$\mathbf{M}_l[n|n] = (\mathbf{I} - \boldsymbol{\Gamma}_l[n]\mathbf{F}_l[n])\,\mathbf{M}[n|n-1]. \tag{14}$$

B. Signal Processing at the FC

The L sensor nodes then communicate their respective filtered estimates, and the corresponding error covariance matrices to the FC via the back haul link. The FC treats these estimates as its observations, to construct the vector

$$\mathbf{y}_f[n] = [\hat{\mathbf{s}}_1^T[n|n], \ldots, \hat{\mathbf{s}}_L^T[n|n]]^T, \tag{15}$$

that can be expressed as,

$$\mathbf{y}_f[n] = \mathbf{B}\mathbf{s}[n] + \mathbf{w}_{y,f}[n], \tag{16}$$

where $\mathbf{B} = \mathbf{1}_L \otimes \mathbf{I}_4$, with $\mathbf{1}_L$ representing a length L vector containing all 1s, and $\mathbf{w}_{y,fc}$ is the observation noise due to the sensor estimation error, and back-haul AWGN, such that $\mathbf{w}_{y,fc}[n] \sim \mathcal{CN}(\mathbf{0}, \mathbf{R}_{y,f})$ where $\mathbf{R}_{y,f}$ is a $4L \times 4L$ block diagonal matrix, containing L 4×4 blocks, such that its lth block is given as $(\mathbf{R}_{y,f})_{l,l} = \mathbf{M}_l[n|n] + \sigma_f^2\mathbf{I}_4$, with σ_f^2 being the noise variance for the sensor to FC link.

Now, letting

$$\hat{\mathbf{y}}_f[n|n-1] = \mathbf{B}\hat{\mathbf{s}}[n|n-1], \tag{17}$$

the innovation component at the FC can be calculated as

$$\boldsymbol{\alpha}_f[n] = \mathbf{y}_f[n] - \hat{\mathbf{y}}_f[n|n-1], \tag{18}$$

and its covariance matrix can be obtained as

$$\mathbf{R}_{\alpha,f}[n] = \mathbf{B}\mathbf{M}[n|n-1]\mathbf{B}^H + \mathbf{R}_{y,f}. \tag{19}$$

The Kalman filter gain at the FC hence takes the form,

$$\begin{aligned}\boldsymbol{\Gamma}_f[n] &= \left(E[\mathbf{s}[n]\boldsymbol{\alpha}_f^H[n]]\right)\mathbf{R}_{\alpha,f}^{-1}[n] \\ &= (\mathbf{M}[n|n-1]\mathbf{B}^H)(\mathbf{B}\mathbf{M}[n|n-1]\mathbf{B}^H + \mathbf{R}_{y,f})^{-1}.\end{aligned} \tag{20}$$

Based on these, the filtered state vector at the nth adaptation cycle takes the form

$$\hat{\mathbf{s}}[n|n] = \hat{\mathbf{s}}[n|n-1] + \boldsymbol{\Gamma}_f[n]\boldsymbol{\alpha}_f, \tag{21}$$

and $\mathbf{M}[n|n]$ can be updated as

$$\mathbf{M}[n|n] = (\mathbf{I} - \boldsymbol{\Gamma}_f[n]\mathbf{B})\mathbf{M}[n|n-1]. \tag{22}$$

IV. Communications Operation

As stated earlier, the communications frame is divided into two subframes, viz. channel estimation and uplink data transmission. In this section we look at the operations performed at the APs and at the CPU during these two subframes.

A. The Channel Estimation Sub-frame

Let the kth UE transmit a pilot signal ψ_k such that $\sum_{n=1}^{K}\psi_k[n]\psi_l^*[n] = \rho_{kl}$, with $0 \le |\rho_{kl}| \le 1$ representing the correlation coefficient between the pilot sequences transmitted by the kth and the lth users. Consequently, the signal vector received by the CPU at the nth instant can be expressed as

$$\mathbf{z}[n] = \sum_{k=1}^{K}\sqrt{\epsilon_{p,k}}\psi_k[n]\mathbf{h}_k + \mathbf{G}_r\boldsymbol{\zeta}[n] + \mathbf{w}[n], \tag{23}$$

where $\mathbf{z}[n] = [\mathbf{z}_1^T[n], \mathbf{z}_2^T[n], \ldots, \mathbf{z}_N^T[n]]^T$, $\mathbf{h}_k = [\sqrt{\beta_{k1}}\mathbf{h}_{k1}^T, \sqrt{\beta_{k2}}\mathbf{h}_{k2}^T, \ldots, \sqrt{\beta_{kN}}\mathbf{h}_{kN}^T]^T$, $\epsilon_{p,k}$ is the uplink transmit pilot power corresponding to kth user, $\mathbf{G}_r = [\mathbf{G}_{r1}^T, \mathbf{G}_{r2}^T, \ldots, \mathbf{G}_{rN}^T]^T$ and $\mathbf{w}[n] = [\mathbf{w}_1^T[n], \mathbf{w}_2^T[n], \ldots, \mathbf{w}_N^T[n]]$. It is easy to show that $\mathbf{h}_k \sim \mathcal{CN}(\mathbf{0}, (\boldsymbol{\beta}_k \otimes \mathbf{1}_{M_aN\times Ma}) \odot \mathbf{R}_k)$, with $\mathbf{R}_k \in \mathcal{C}^{M_aN\times M_aN}$ being a block diagonal matrix whose ith block is given as $(\mathbf{R}_k)_{ii} = \mathbf{R}_{ki}$, and $\boldsymbol{\beta}_k = [\beta_{k1}, \ldots, \beta_{kN}]$. We can now define

$$\mathbf{z}_l \triangleq \sum_{n=1}^{K}\mathbf{z}[n]\psi_l[n]. \tag{24}$$

The CPU may or may not have the phase synchronization information about $\boldsymbol{\zeta}[n]$. In the former case, the CPU can form $\mathbf{z}_l^{'}$ by subtracting $\sum_{n=1}^{K}\hat{\mathbf{G}}_r\boldsymbol{\zeta}[n]\psi_l[n]$ from $\mathbf{z}_l$ to obtain the vector $\mathbf{z}_l^{'}$. In this case, using the results derived in [21], we can show that the LMMSE estimate of $\mathbf{h}_k$ at the CPU can be expressed as

$$\hat{\mathbf{h}}_{\mathbf{k}} = \boldsymbol{\Sigma}_{hz,k}\boldsymbol{\Sigma}_{z^{'}z^{'},k}^{-1}\mathbf{z}_k^{'}, \tag{25}$$

where $\boldsymbol{\Sigma}_{hz,k} = \sqrt{\epsilon_{p,k}}(\boldsymbol{\beta}_k \otimes \mathbf{1}_{M_aN\times Ma}) \odot \mathbf{R}_k$ and $\boldsymbol{\Sigma}_{z^{'}z^{'},k} = E[\mathbf{z}_k^{'}\mathbf{z}_k^{'H}]$ is a block diagonal matrix whose ith block is given as

$$\begin{aligned}(\boldsymbol{\Sigma}_{z^{'}z^{'},k})_{ii} = \epsilon_{p,k}\beta_{ki}\mathbf{R}_{ki} + \sum_{\substack{n=1,\\ l\neq k}}^{K}\rho_{nk}^2\epsilon_{p,n}\beta_{ni}\mathbf{R}_{ni} \\ + (P_tN_t\eta_{ei} + N_0)\mathbf{I}_{M_a}.\end{aligned} \tag{26}$$

It is easy to show that the covariance matrix of $\hat{\mathbf{h}}$ can be expressed as

$$\bar{\mathbf{R}}_k^{'} = \boldsymbol{\Sigma}_{hz,k}\boldsymbol{\Sigma}_{z^{'}z^{'},k}^{-1}\boldsymbol{\Sigma}_{hz,k}^H. \tag{27}$$

and the covariance matrix of $\tilde{\mathbf{h}}_k$ is given by

$$\dot{\mathbf{R}}_k^{'} = (\boldsymbol{\beta}_k \otimes \mathbf{1}_{M_aN\times Ma}) \odot \mathbf{R}_k - \bar{\mathbf{R}}_k^{'}. \tag{28}$$

Similarly, in case the synchronization information about $\boldsymbol{\zeta}[n]$ is not available at the CPU, then $\hat{\mathbf{h}}_k$ becomes

$$\hat{\mathbf{h}}_{\mathbf{k}} = \boldsymbol{\Sigma}_{hz,k}\boldsymbol{\Sigma}_{zz,k}^{-1}\mathbf{z}_k, \tag{29}$$

and $\boldsymbol{\Sigma}_{zz,k} = E[\mathbf{z}_k\mathbf{z}_k^H]$ is a block diagonal matrix whose ith block is given as

$$\begin{aligned}(\boldsymbol{\Sigma}_{zz,k})_{ii} = \epsilon_{p,k}\beta_{ki}\mathbf{R}_{ki} + \sum_{\substack{n=1,\\ l\neq k}}^{K}\rho_{nk}^2\epsilon_{p,n}\beta_{ni}\mathbf{R}_{ni} + P_t\hat{\mathbf{G}}_{ri}\hat{\mathbf{G}}_{ri}^H + \\ (P_tN_t\eta_{ei} + N_0)\mathbf{I}_{M_a}.\end{aligned} \tag{30}$$

In this case, the covariance matrix of $\hat{\mathbf{h}}$ takes the form

$$\bar{\mathbf{R}}_k = \boldsymbol{\Sigma}_{hz,k}\boldsymbol{\Sigma}_{zz,k}^{-1}\boldsymbol{\Sigma}_{hz,k}^H. \quad (31)$$

Now, $\mathbf{h}_k$ can be expressed in terms of $\hat{\mathbf{h}}_{\mathbf{k}}$ and an orthogonal estimation error component $\tilde{\mathbf{h}}_k$ as $\mathbf{h}_k = \hat{\mathbf{h}}_k + \tilde{\mathbf{h}}_k$, with $E[\hat{\mathbf{h}}_k\tilde{\mathbf{h}}_k^H]$ being an order MN all zero square matrix, $\tilde{\mathbf{h}}_k$ being a ZMCSCG random vector whose covariance matrix is

$$\dot{\mathbf{R}}_k = (\boldsymbol{\beta}_k \otimes \mathbf{1}_{M_aN\times Ma}) \odot \mathbf{R}_k - \bar{\mathbf{R}}_k. \quad (32)$$

B. Data Transmission

The received signal at the CPU in the presence of radar interference can be written as

$$\mathbf{z}[n] = \sum_{l=1}^{K}\sqrt{\epsilon_{x,l}}x_l[n]\hat{\mathbf{h}}_l + \sum_{l=1}^{K}\sqrt{\epsilon_{x,l}}x_l[n]\tilde{\mathbf{h}}_l + \hat{\mathbf{G}}_r\boldsymbol{\zeta}[n] + \tilde{\mathbf{G}}_r\boldsymbol{\zeta}[n] + \sqrt{N_0}\mathbf{w}_z[n] \quad (33)$$

Now, based on the available channel estimates, the CPU can construct the MMSE combining vector corresponding to the kth UE as, $\mathbf{v}_k = \mathbf{R}_{z|\hat{\mathbf{H}},\hat{\mathbf{G}}_r}^{-1}\hat{\mathbf{h}}_k$, where $\mathbf{R}_{z|\hat{\mathbf{H}},\hat{\mathbf{G}}_r}$ is the covariance matrix of $\mathbf{z}[n]$ given the channel estimates $\hat{\mathbf{H}}$ and $\hat{\mathbf{G}}_r$ [16]. This can be expressed as,

$$\mathbf{R}_{z|\hat{\mathbf{H}},\hat{\mathbf{G}}_r} = \sum_{l=1}^{K}\epsilon_{x,l}\left(\hat{\mathbf{h}}_l\hat{\mathbf{h}}_l^H + \dot{\mathbf{R}}_l^{'}\right) + P_t(\hat{\mathbf{G}}_{\mathbf{r}}\hat{\mathbf{G}}_{\mathbf{r}}^H + \mathbf{I}_{M_a}\otimes \mathrm{diag}(\boldsymbol{\eta}_e)) + N_0\mathbf{I}_{M_aN}, \quad (34)$$

where $\boldsymbol{\eta}_e = [\eta_{e,1},\ldots,\eta_{e,N}]^T$. Consequently, the processed signal vector corresponding to the kth UE, $\mathbf{r}_k[n] = \mathbf{v}_k^H\mathbf{z}[n]$, at the nth instant takes the form

$$\mathbf{r}_k[n] = \sqrt{\epsilon_{x,k}}\hat{\mathbf{h}}_k^H\mathbf{R}_{z|\hat{\mathbf{H}},\hat{\mathbf{G}}_r}^{-1}\hat{\mathbf{h}}_kx_k[n] + \sum_{\substack{l=1,\\ l\neq k}}^{K}\sqrt{\epsilon_{x,l}}\hat{\mathbf{h}}_k^H\mathbf{R}_{z|\hat{\mathbf{H}},\hat{\mathbf{G}}_r}^{-1}\hat{\mathbf{h}}_lx_l[n] + \sum_{l=1}^{K}\sqrt{\epsilon_{x,l}}\hat{\mathbf{h}}_k^H\mathbf{R}_{z|\hat{\mathbf{H}},\hat{\mathbf{G}}_r}^{-1}\tilde{\mathbf{h}}_lx_l[n] + \hat{\mathbf{h}}_k^H\mathbf{R}_{z|\hat{\mathbf{H}},\hat{\mathbf{G}}_r}^{-1}\hat{\mathbf{G}}_r\mathbf{r}[n] + \hat{\mathbf{h}}_k^H\mathbf{R}_{z|\hat{\mathbf{H}},\hat{\mathbf{G}}_r}^{-1}\tilde{\mathbf{G}}_r\mathbf{r}[n] + \sqrt{N_0}\hat{\mathbf{h}}_k^H\mathbf{R}_{z|\hat{\mathbf{H}},\hat{\mathbf{G}}_r}^{-1}\mathbf{w}_z[n]. \quad (35)$$

Based on this, the rate achievable by the kth user in the uplink can be expressed as [16]

$$\mathbf{R}_k = \log_2(1+\gamma_k) \quad (36)$$

where γ_k is the SINR for the kth user's signal at the CPU and is given as (37).

V. Numerical Results

In this section we validate our derived results using Monte-Carlo simulations. Here, the communication subsystem consists of a CF-mMIMO system spread over a circular region with a radius 500 m. We assume both the APs and the users to be distributed uniformly across the cell, and operating at a carrier frequency f_c = 3 GHz. Both the communications and the radar signals are assumed to have a bandwidth of 20 MHz. In this setup, unless stated otherwise, we consider K=16 users and $N = 256$ APs. The channel covariance matrices at all the APs is $\boldsymbol{\Sigma}_k$ is assumed to be identity. The communication frame consists of 1024 channel uses with the first K channel uses dedicated for training, ensuring orthogonal pilots, and the remaining for uplink data transmission. For the purpose of these experiments, we consider the interference channels to be known at the APs with a 10% error, and the median received SNR for the communications subsystem to be 20 dB. The large scale fading coefficients of the wireless channel (β_{ik}) are modelled as $\beta_{ik} = \min\left(1, \left(\frac{d_{ik}}{d_0}\right)^{-\eta}\right)$ with d_{ik} being the distance between the ith AP and the kth UE, and $\eta = 3.6$.

On the other hand, the radar subsystem consists of a multi-static radar comprising a transmitter with $M_t = 8$ antennas and L single antenna sensors. The radar sensors are also assumed to be uniformly distributed across the cell. All the performance metrics presented in this section are generated by averaging over 10,000 realizations of the system.

Fig. 2 plots the mean square error (MSE) of the estimate of radar target parameter as a function of iteration count for different number of radar sensors (L) when the median received radar SNR is 20 dB for K=16. As expected, the MSE decreases almost linearly with an the increase in L.

To investigate the impact of number of communication users over the performance of the radar, Fig. 3 plots the mean square error (MSE) of the estimate of radar target parameter as a function of number of communication users for different number of radar sensors (L) at the 50th iteration for a median received radar SNR of 20 dB. We observe a marginal increase in the MSE with an increase in K.

Fig. 4 plots the achievable per user uplink rate as a function of the AP density for different radar received SNRs. We observe that similar to the radar subsystem, the increase in the radar transmit power minimally affects the performance of the communications subsystem.

VI. Conclusions

In this paper, we analysed the coexistence of a cell free massive MIMO communication system with a tracking multi-static radar system. We observed that the radar performance improves significantly with the increase in the number of radar sensors and also observed that the impact of communication

$$\gamma_k = \frac{\epsilon_{x,k}|\mathbf{v}_k^H\hat{\mathbf{h}}_k|^2}{\sum_{\substack{l=1,\\ l\neq k}}^{K}\epsilon_{x,l}|\mathbf{v}_k^H\hat{\mathbf{h}}_l|^2 + \sum_{l=1}^{K}\epsilon_{x,l}\mathbf{v}_k^H\dot{\mathbf{R}}_l\mathbf{v}_k + P_t\mathbf{v}_k^H(\hat{\mathbf{G}}_{\mathbf{r}}\hat{\mathbf{G}}_{\mathbf{r}}^H + \boldsymbol{\eta}_e\otimes\mathbf{I}_{M_a})\mathbf{v}_k + N_0\mathbf{v}_k^H\mathbf{v}_k} \quad (37)$$

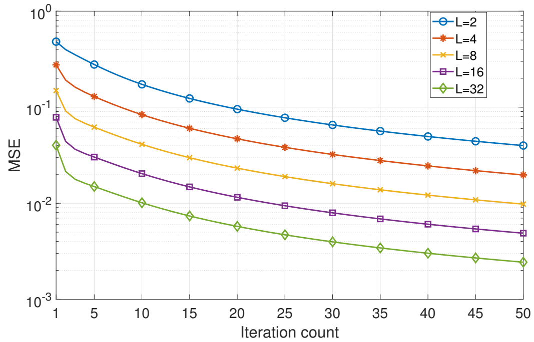

Fig. 2: Convergence performance of tracking radar for different numbers of radar sensors (L).

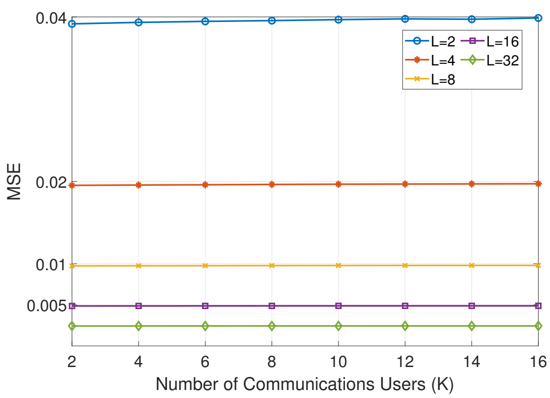

Fig. 3: Tracking MSE for different numbers of communication users (K).

system interference over radar system performance is negligible. Similarly, we observed that the performance of the communications subsystem remains largely unaffected by the radar transmit power. This confirms our hypothesis that multistatic radars can coexist with cell free massive MIMO without co-design.

ACKNOWLEDGMENT

This work was supported by SERB-METRICS vide grant number MTR/2023/000498.

REFERENCES

[1] United States Department of Transportation, NHTSA, "Automated vehicles for safety," n.d., accessed Dec 11, 2020. https://www.nhtsa.gov/technology-innovation/automated-vehicles-safety.

[2] M. Labib, V. Marojevic, A. F. Martone, J. H. Reed, and A. I. Zaghloui, "Coexistence between communications and radar systems: A survey," *URSI Radio Science Bulletin*, vol. 2017, no. 362, pp. 74–82, 2017.

[3] F. Liu, Y. Cui, C. Masouros, J. Xu, T. X. Han, Y. C. Eldar, and S. Buzzi, "Integrated sensing and communications: Toward dual-functional wireless networks for 6g and beyond," *IEEE Journal on Selected Areas in Communications*, vol. 40, no. 6, pp. 1728–1767, 2022.

[4] L. Yin, Z. Liu, M. Alaee-Kerahroodi, B. Clerckx *et al.*, "Integrated sensing and communications enabled low earth orbit satellite systems," *arXiv preprint arXiv:2304.00941*, 2023.

[5] F. Liu, C. Masouros, A. P. Petropulu, H. Griffiths, and L. Hanzo, "Joint radar and communication design: Applications, state-of-the-art, and the road ahead," *IEEE Transactions on Communications*, vol. 68, no. 6, pp. 3834–3862, 2020.

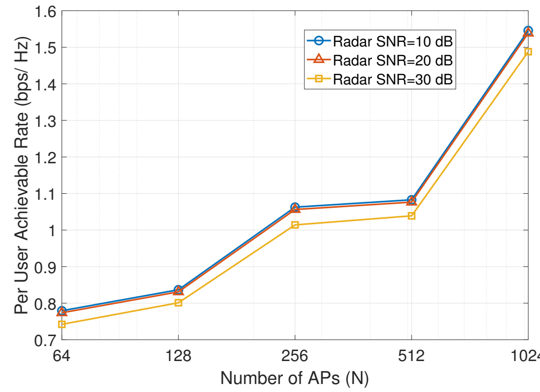

Fig. 4: Uplink achievable rate for different number of serving APs (N).

[6] A. R. Chiriyath, B. Paul, and D. W. Bliss, "Radar-communications convergence: Coexistence, cooperation, and co-design," *IEEE Transactions on Cognitive Communications and Networking*, vol. 3, no. 1, pp. 1–12, 2017.

[7] C. D'Andrea, S. Buzzi, and M. Lops, "Communications and radar coexistence in the massive mimo regime: Uplink analysis," *IEEE Transactions on Wireless Communications*, vol. 19, no. 1, pp. 19–33, 2020.

[8] A. Mishra and R. Chopra, "MIMO radars and massive MIMO communication systems can coexist," *CoRR*, vol. abs/2304.00890, 2023. [Online]. Available: https://doi.org/10.48550/arXiv.2304.00890

[9] R. Saruthirathanaworakun, J. M. Peha, and L. M. Correia, "Opportunistic sharing between rotating radar and cellular," *IEEE Journal on Selected Areas in Communications*, vol. 30, no. 10, pp. 1900–1910, 2012.

[10] A. Khawar, A. Abdelhadi, and C. Clancy, "Target detection performance of spectrum sharing mimo radars," *IEEE Sensors Journal*, vol. 15, no. 9, pp. 4928–4940, 2015.

[11] A. R. Chiriyath, B. Paul, G. M. Jacyna, and D. W. Bliss, "Inner bounds on performance of radar and communications co-existence," *IEEE Transactions on Signal Processing*, vol. 64, no. 2, pp. 464–474, 2015.

[12] T. L. Marzetta, *Fundamentals of massive MIMO*. Cambridge University Press, 2016.

[13] A. Sakhnini, M. Guenach, A. Bourdoux, H. Sahli, and S. Pollin, "A target detection analysis in cell-free massive mimo joint communication and radar systems," in *ICC 2022 - IEEE International Conference on Communications*, 2022, pp. 2567–2572.

[14] M. Alaee-Kerahroodi, E. Raei, S. Kumar, and B. S. M. R. R., "Cognitive radar waveform design and prototype for coexistence with communications," *IEEE Sensors Journal*, vol. 22, no. 10, pp. 9787–9802, 2022.

[15] H. Q. Ngo, A. Ashikhmin, H. Yang, E. G. Larsson, and T. L. Marzetta, "Cell-free massive mimo versus small cells," *IEEE Transactions on Wireless Communications*, vol. 16, no. 3, pp. 1834–1850, 2017.

[16] S. Mukherjee and R. Chopra, "Performance analysis of cell-free massive mimo systems in los/ nlos channels," *IEEE Transactions on Vehicular Technology*, vol. 71, no. 6, pp. 6410–6423, 2022.

[17] X. Wang, D. Musicki, R. Ellem, and F. Fletcher, "Efficient and enhanced multi-target tracking with doppler measurements," *IEEE Transactions on Aerospace and Electronic Systems*, vol. 45, no. 4, pp. 1400–1417, 2009.

[18] L. Wu, K. V. Mishra, M. R. B. Shankar, and B. Ottersten, "Resource allocation in heterogeneously-distributed joint radar-communications under asynchronous bayesian tracking framework," *IEEE Journal on Selected Areas in Communications*, vol. 40, no. 7, pp. 2026–2042, 2022.

[19] M. I. Skolnik, "Theoretical accuracy of radar measurements," *IRE Transactions on Aeronautical and Navigational Electronics*, vol. ANE-7, no. 4, pp. 123–129, 1960.

[20] P. Z. Peebles, *Radar principles*. John Wiley & Sons, 2007.

[21] E. Björnson, J. Hoydis, L. Sanguinetti *et al.*, "Massive mimo networks: Spectral, energy, and hardware efficiency," *Foundations and Trends® in Signal Processing*, vol. 11, no. 3-4, pp. 154–655, 2017.